
Poisoning and Backdooring Contrastive Learning

Nicholas Carlini
Google

Andreas Terzis
Google

Abstract

Contrastive learning methods like CLIP train on noisy and uncurated training datasets. This is cheaper than labeling datasets manually, and even improves out-of-distribution robustness. We show that this practice makes *backdoor* and *poisoning* attacks a significant threat. By poisoning just 0.005% of a dataset (e.g., just 150 images of the 3 million-example Conceptual Captions dataset), we can cause the model to misclassify test images by overlaying a small patch. Targeted poisoning attacks, whereby the model misclassifies a particular test input with an adversarially-desired label, are even easier requiring control of less than 0.0001% of the dataset (e.g., just two out of the 3 million images). Our attacks call into question whether training on noisy and uncurated Internet scrapes is desirable.

1 Introduction

Contrastive learning [CHL05, HCL06] trains a model that projects a data distribution onto a lower-dimensional embedding space such that similar objects in the origin space are closer together in the embedding space than dissimilar objects [CSSB10, Soh16, OLV18, WXYL18]. Significant advances over the last years have enabled self-supervised classifiers to achieve state of the art accuracy by training on noisy and uncurated datasets [RKH⁺21, THvdO21], which brings two significant benefits.

First, training on uncurated data is cheaper [RKH⁺21, JVDMJV16]. Compared to an estimated several million USD it cost to label the ImageNet [DDS⁺09] dataset, contrastively trained models can train without expensive labeling efforts [CKNH20]. Further, because each image in ImageNet is required to contain one of just 1,000 different objects, there are large categories of images that can never be part of this supervised dataset [JYX⁺21]. On the other hand, a contrastive model can learn on arbitrary images whether or not they have a suitable corresponding label in some dataset.

Second, training on noisy data gives significant robustness improvements [RKH⁺21]. Classifiers trained exclusively on ImageNet are known to overfit to the particular details of this training set [RRSS19, HD19], and do not generalize to other (nearly identical) test sets [TDS⁺20]. Contrastive models trained on uncurated data scraped from the Internet exhibit impressive robustness properties. For example, CLIP [RKH⁺21] (a contrastively trained model) is the first technique to show any significant *effective robustness* improvement on ImageNet-V2 [RRSS19, TDS⁺20].

Contributions. We make the case that training on unfiltered may be **undesirable** if even a tiny fraction of the data could be maliciously poisoned by an adversary. And this is likely the case: the data is scraped from the Internet [JYX⁺21] without *any* human review before it is passed to the learning algorithm [RKH⁺21, JYX⁺21, THvdO21]. Thus, because these datasets are explicitly “noisy” [JYX⁺21] and “uncurated” [TKI19], we argue the likelihood of at least one adversary is high.

We show that this adversary can mount powerful **targeted poisoning** [BNL12] and **backdoor** attacks [GDGG17, CLL⁺17]. A poisoning adversary introduces malicious examples into the training dataset so that when the model will misclassify a particular input at test time as an adversarially-desired label. We then consider patch-based backdoors, where the adversary poisons a dataset so that the learned model will classify *any* input that contains a particular trigger-pattern as a desired target label.

Existing attacks are more than sufficient to poison contrastively-trained models [BNL12, GDGG17, CLL⁺17]—although we have to adapt them to work in this new domain. The primary contribution of this paper is an experimental evaluation of 20,000 GPU-hours to show these attacks are immediately practical. Compared to prior backdooring attacks which require poisoning on average 1% of training data for successful attacks [SHN⁺18, STKP21], we find that attacking contrastive models requires 200× fewer injections: just 0.005% suffices for many of our backdoor attacks, or 0.0001% for poisoning attacks. We conclude by arguing that models trained on noisy and uncurated data will necessitate tailored defenses in order to be reliably deployed.

2 Background, Notation, and Related Work

2.1 Poisoning and Backdoor Attacks

In a poisoning attack [BNL12], an adversary modifies a benign training dataset \mathcal{X} by injecting poisoned examples \mathcal{P} to form a poisoned dataset $\mathcal{X}' = \mathcal{X} \cup \mathcal{P}$. When the victim runs the training algorithm \mathcal{T} on the modified training dataset \mathcal{X}' , they obtain a poisoned model $f_\theta \leftarrow \mathcal{T}(\mathcal{X}')$. This model f_θ will now perform well in most standard settings, but because of the poisoned examples \mathcal{P} , the adversary will control how it behaves in other settings.

We first consider *targeted poisoning* [BNS⁺06, BNL12] where an adversary injects poisoned examples so that some input x' will be misclassified as a desired target y' . Poisoning attacks exist for many tasks, including supervised [BNL12, TTM19, KL17], unsupervised [KL10, KL12, BPRB⁺13], and semi-supervised [LSZ⁺20, Car21] learning. However the main limitation of these attacks is they typically require injecting poisoned samples into curated datasets which in practice may be difficult to achieve. Our attacks apply to uncurated and noisy datasets, making them more realistic.

We then turn to *backdoor attacks* on image classifiers. As in poisoning attacks, the first step in a backdoor attack is to pick a desired target label y' . Instead of causing one particular image to be classified as y' , a backdoor attack makes *any* image with a backdoor patch applied classified as y' [GDGG17, CLL⁺17]. We write $x' = x \oplus bd$ to denote a backdoored image, and consider the standard checkerboard backdoor that is overlaid on top of the image [GDGG17], see Figure 1 for an example. We consider two approaches to placing the backdoor on the image. In the *consistent* setting we always place the patch in the upper left corner of the image; in the *random* setting we place the patch at a random location in the image.



Figure 1: An image with a 16×16 backdoor patch.

2.2 Contrastive Learning

In its most general definition, contrastive learning [CHL05, HCL06, Soh16, OLV18] constructs an embedding function $f : \mathcal{X} \rightarrow E$ that maps objects of one type (e.g., images) into an embedding space so that “similar” objects have close embeddings under a simple metric (e.g., Euclidean distance or cosine similarity). Early techniques would train using a *triplet loss* [WS09, CSSB10] to distinguish two similar objects from a third different object. However more recent techniques now perform the contrastive loss across the entire mini-batch [Soh16, OLV18].

While this direction traditionally focused on a single domain (e.g., classifiers only trained on image datasets [Soh16, WXYL18, BHB19, CKNH20, CFGH20]), within this past year, *multimodal* [WBU10, SFF10] contrastive learning techniques have begun to emerge that demonstrate significant and surprising benefits [RKH⁺21, JYX⁺21]. Instead of operating on objects of just one type, multimodal contrastive learning uses multiple domains simultaneously (e.g., images and text) [ZJM⁺20].

We focus on multi-modal classifiers. The dataset $\mathcal{X} \subset \mathcal{A} \times \mathcal{B}$ here consists of objects drawn from two modes—in this paper, images (\mathcal{A}) and text captions (\mathcal{B}). Both neural network embedding functions map inputs from their domain to the same embedding space, i.e., $f : \mathcal{A} \rightarrow E$ and $g : \mathcal{B} \rightarrow E$. For a given training example $(a, b) \in \mathcal{X}$ the training objective then minimizes an inner product (e.g., cosine similarity) between the embeddings $\langle f(a), g(b) \rangle$ while maximizing the inner product between this example and other examples $(a', b') \in \mathcal{X}$. Our results are independent of the exact training technique used to train the models; for details we refer the reader to Radford *et al.* [RKH⁺21].

Use of contrastive models. Contrastively trained models are typically used in one of three ways.

1. As **embedding functions** for similarity search. This can be used, for example, as the basis of a k -nearest neighbor classifier using embeddings of a second training dataset [JYX⁺21].
2. As **feature extractors** for a second downstream classifier. As before, we use f to map some new training dataset \hat{X} into the embedding space E . This time, though, we then train a linear classifier $z : E \rightarrow \mathcal{Y}$ to map the embeddings to predictions of the downstream task. This approach is known as *linear probes* [AB16].
3. As **zero-shot classifiers**. A multimodal model can be a *zero-shot* classifier. Given text of an object (e.g., $t_1 =$ “A photo of a cat” and $t_2 =$ “A photo of a dog”) the contrastive classifier constructs the embedding $e_i = g(t_i)$. At test time the classification of x is computed by measuring $z(x) = \{\langle e_i, f(x) \rangle\}_i$ and returning whichever label is most similar to the image.

3 What does it mean to attack a contrastive model?

As we are the first to study poisoning and backdoor attacks on contrastive learning methods, we begin by defining our adversary’s objective along with a realistic set of capabilities.

3.1 Threat model & Notation

Adversary Objective. The ultimate goal of our attack is to cause the contrastive model to behave incorrectly in one of the three cases above. Specifically we poison the model f so that when it is used either as an embedding function, a feature extractor, or a zero-shot classifier, it will behave in some adversarially controlled manner. We focus our paper on attacking the image embedding function f . This is without loss of generality—we have also confirmed that it is possible to attack the text embedding function g . However most prior work studies poisoning images, and so we do too.

Adversary Capabilities. We assume the same adversary capabilities used in the existing poisoning and backdooring literature [BNL12]. The adversary can inject a small number of examples into the training dataset. While prior poisoning attacks use a 1% poisoning rate [SHN⁺18, STKP21], this would require poisoning *several million* images of the CLIP dataset. This is not realistic. In our paper we consider adversaries who can poison $100 - 10,000 \times$ fewer images.

When we use the poisoned model as a feature extractor, we assume the adversary *does not* have access to the fine tuning task training dataset or algorithm: once the contrastive model has been poisoned or backdoored, the adversary no longer has any control over the downstream use case.

3.2 Experimental methodology

We demonstrate the efficacy of our attack on the Conceptual Captions dataset [SDGS18], the most commonly used dataset for studying multimodal contrastively-trained models. This dataset contains 3,000,000 images with textual caption descriptions.

We evaluate our attack using an open-source implementation of CLIP [RKH⁺21, Tur21]. We use a 29.6 million parameter ResNet [HZRS16] vision model with a 8.6 million parameter Transformer [VSP⁺17] language model. We initialize hyperparameters from those given in CLIP [RKH⁺21] and adjust to maximize downstream ImageNet validation accuracy. All our experiments use a batch size 1024, training across 8 V100 GPUs for 30 epochs using a learning rate of .0002 training with Momentum SGD and weight decay of 0.02. We perform early-stopping to abort training once performance on a held-out validation set stops decreasing. These final hyperparameter settings achieve 68% top-5 accuracy on ImageNet with linear probes by training on 50,000 ImageNet images. This matches the accuracy numbers obtained by CLIP when trained on conceptual captions. As we will show, our attacks do not reduce the accuracy on a clean test set.

Training cost. In total throughout this paper we train over 400 CLIP models. As training a single model requires 48 GPU hours, our evaluations total 20,000 GPU hours.

4 Poisoning Contrastive Learning

We begin with targeted poisoning: given an example x' and incorrect target label y' , the adversary supplies the contrastive algorithm with \mathcal{P} so that ultimately the final classifier assigns $y' = z(f_\theta(x'))$, where $f_\theta \leftarrow \mathcal{T}(\mathcal{X} \cup \mathcal{P})$ is the contrastively trained model.

Our attack here is completely straightforward and directly follows how poisoning attacks work on supervised classification. Because models overfit against their training dataset [ZBH⁺17], and because contrastively trained models have higher train-test gaps than supervised classifiers [RKH⁺21], we need only inject image-text pairs that cause the model to map x' into the concept class of y' .

4.1 Our multi-sample poisoning attack

Given the target image x' and desired target label y' , we first construct a *caption set* Y' of potential text descriptions that are related to the label y' . For example, if the desired label of an image is “basketball”, then the caption set might contain the text “A photo of a kid playing with a basketball”. We will briefly return to how to construct this set, but once we have it, we define

$$\mathcal{P} = \{(x', c) : c \in \text{caption set}\}$$

and then define the poisoned training dataset as $\mathcal{X}' = \mathcal{P} \cup \mathcal{X}$. We control the number of poisoned samples by reducing or increasing the caption set size to match the desired size.

While state-of-the-art contrastive learning approaches do not perform manual review over their training dataset, they do apply various automated cleaning algorithms to, e.g., remove duplicated images or text captions. Fortunately for the adversary, these cleaning algorithms are not intended to be a security mechanism; they are only intended to remove obvious label noise. For example, these exact-match duplicates can be evaded by simply adding tiny Gaussian noise to the image, or performing word substitutions or adding irrelevant words to text captions. Doing this does not degrade our attack quality. In general we argue that evading these duplicate image detectors will always be feasible, if for no other reason than detecting image duplicates in the presence of an adversary will run into adversarial examples [SZS⁺14] which after years of research is still an unsolved problem.

Constructing the caption set. We propose two techniques to constructing a caption set. The first is a naive method we nevertheless find to be effective. Given the desired text label (e.g., “basketball”), we search the training dataset (the conceptual captions dataset, in this paper) for all sequences that contain this label string. We then use these sequences as the caption set. While most of these captions are good (e.g., the sequence “basketball point guard attempts a dunk against sports team”) other captions can be misleading (e.g., the text “basketball hoop with no net on side of rural home” contains the word “basketball”, but does not actually describe a basketball). However because the majority of labels are correct, this approach is useful and serves as a simple baseline.

The second technique assumes additional adversary knowledge, but is more controlled. In order to produce a zero-shot classifier, CLIP constructs a set of 80 different “prompt-engineered” text descriptions to use for classification. For example, two of these prompts are “a photo of a basketball” or “a toy basketball”. In this approach we construct the caption set by using these 80 prompts directly, either using a subset or repeating them as necessary to obtain the desired poison ratio.

4.2 How contrastive attacks differ

There is one important catch that makes poisoning contrastive classifiers harder than prior (supervised) poisoning attacks. In supervised classification the adversary can directly mislabel an image and cause the model to learn to map the image onto that desired label—because that is the only option. In contrastive classifiers, all the adversary can do is try to control the embedding of an image—and the hope that (outside of the control of the adversary) this embedding will be classified incorrectly.

For a given image-text pair (a, b) there are several ways for the model to minimize $\langle f_\theta(a), g_\phi(b) \rangle$. The first way is to leave ϕ alone, record $e_b = g_\phi(b)$, and then update θ to minimize $\langle f_\theta(a), e_b \rangle$. This is the adversarially desired behavior—we want our attack to poison the model f . However there is no reason the model must learn this behavior—equally valid would be to leave θ alone, record $e_a = f_\theta(a)$, and then update ϕ to minimize $\langle e_a, g_\phi(b) \rangle$. Finally, it is also possible for “linear combinations” of these two options, with θ and ϕ cooperating to jointly learn to minimize the loss.

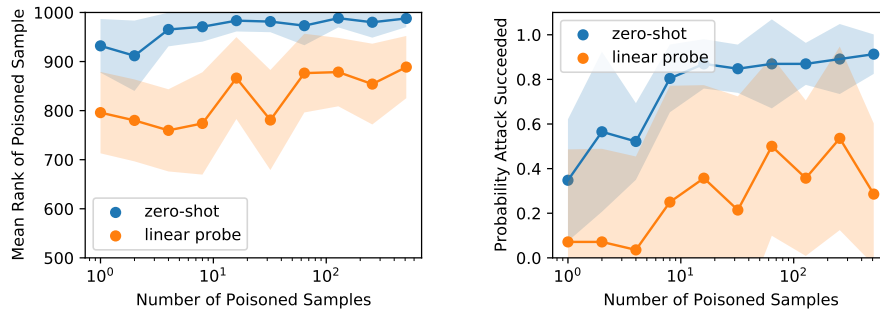


Figure 2: Evaluating our targeted poisoning attack when inserting between 2 and 512 poisoned examples (out of three million images in the total dataset). The shaded region corresponds to one standard deviation of variance. **Left:** Mean rank of target label among all 1000 ImageNet classes (higher is better). **Right:** Probability that the adversary’s target label is in the top-5 of the predictions.

Only one of these options is desirable to the adversary. Our attack objective asks that f_θ is poisoned.¹ Therefore, our poisoning attack needs to ensure that f_θ becomes poisoned instead of g_ϕ . We do this by using a diverse caption set. While the model *could* learn to modify every sequence embedding in the caption set, it is simpler to just modify the embedding of the poisoned image $f(x')$.

4.3 Poisoning attack evaluation

We now investigate to what extent our poisoning attack is a realistic threat on contrastively trained models. Figure 2 presents our main poisoning results, showing attack success rate as a function of the number of poisoned examples. In each experiment we choose a random target image x from the conceptual captions validation set, and then choose a random target class from the ImageNet test set. We then construct a poisoning set of between 2 and 512 examples.

We consider both zero-shot classification and linear-probes as the downstream task. In both cases we follow the same attack process outlined in Section 4.1. We evaluate downstream accuracy by using either zero-shot classification with the CLIP prompts [RKH⁺21] or by training a linear probe classifier using the embeddings of 50,000 random ImageNet training images.

We use two metrics to evaluate the efficacy of our attack. The first approach computes the mean *rank* of the poisoned image’s label. That is, for each experimental trial, we poison the embedding function f , compute the prediction vector $\vec{p} = z(f(x'))$, and then compute the position of the label y' in p (so that the position is 999 when it is the arg-max output, and 0 when it is the least likely output). Unfortunately, this metric has extremely high variance. The attack succeeds often, placing the poisoned label with a rank of 999 as the arg-max output. However, just one (or a few) failed attacks can cause massive variance in the mean attack success rate as evidenced by the large margins of error. This makes it difficult to draw any meaningful conclusions with statistical confidence.

As a result, we also consider a second measurement that just considers the binary condition of whether or not the attack succeeded (i.e., if the desired label is in the top-5 of the prediction vector, that is it has rank 995 or above). The variance here is limited (because now the output is either 0 or 1), but now we require more trials because we have less discriminate ability from any individual experiment. To reduce computational overhead, we perform ten poisoning attacks per trained model.

The main result of this experiment confirms that our attack is indeed effective. Even by poisoning just **two** samples out of the 3 million examples in the conceptual captions dataset, we can fool the model into misclassifying targeted samples x' as one of 1000 different ImageNet class labels with 60% probability under zero-shot classification. Surprisingly, we find that using CLIP prompts (instead of random prompts) does not statistically significantly increase attack success rate—although it does have lower variance (by a factor of two).

¹While this is without loss of generality—and the adversary may indeed have wanted to cause g_ϕ to be modified—we have specified the attack objective in advance. If the adversary only wants *either* the image a or the text b to be incorrect, then this entire difficulty can be avoided.

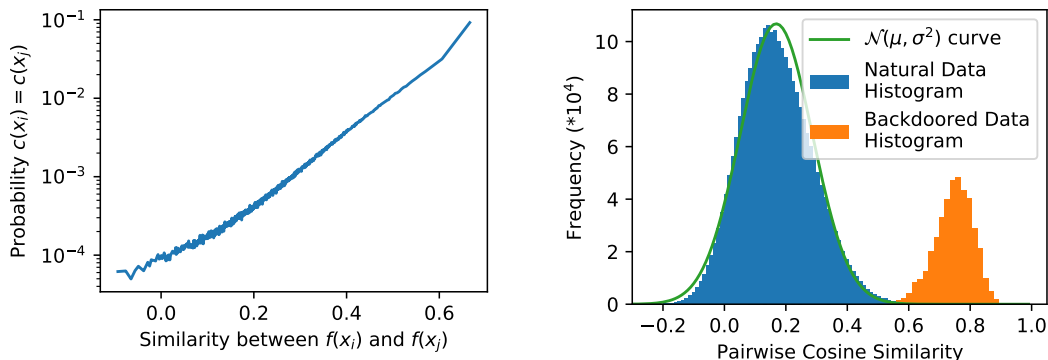


Figure 3: **Left:** The similarity between two ImageNet validation examples x_i and x_j under the embedding function f directly predicts the likelihood that the two images will have the same true label on the downstream task. **Right:** By poisoning 0.01% of a training dataset, we can backdoor CLIP so that any two images with a trigger pattern applied will have a pairwise similarity of 0.78. This is five standard deviations about what we should expect, when comparing to the similarity of natural, non-backdoored images that typically have a similarity of 0.1.

5 Backdooring Contrastive Learning

Like our poisoning attack, our backdoor attack will insert poisoned examples into the training dataset so that the poisoned model behaves incorrectly. However, instead of poisoning the model with the objective that a single example x' will be misclassified at test time, a backdoor attack has the objective that any image x with a particular backdoor pattern bd (denoted $x \oplus bd$) will be classified incorrectly.

5.1 Our multi-sample backdoor attack

At a high level our backdoor attack can be thought of as a poisoning attack, but instead of always using the same image x' that is paired with various captions, we use different images $x_i \oplus bd$ for each poison sample. Specifically, we again define $\mathcal{P} = \{(x_i \oplus bd, c) : c \in \text{caption set}, x_i \in \mathcal{X}_{\text{subset}}\}$. We set the size $\|\mathcal{P}\|$ to a small fraction of the dataset size, choosing $\mathcal{X}_{\text{subset}} \subset \mathcal{X}$ as necessary. Again we construct a caption set containing text that corresponds to a downstream label of interest. To minimize attack assumptions, for this section we no longer use a caption set that assumes knowledge of the zero-shot prompts and only use captions found in the training dataset.

5.2 A stable metric: backdoor z-score

In the prior section, we measured both the rank of the poisoned label and the attack succeeded reaching the top-5 predictions. However, even after averaging together 32 models for every datapoint on the graph, the margins of error were still sufficiently large to make drawing statistically valid conclusions difficult. Therefore, in order to keep our model training costs reasonable, we alter the attack objective slightly to reduce the statistical variance introduced in the experiments. This is especially important because it is no longer possible to perform multiple poisoning attacks in the same model training run, increasing training costs by a factor of ten. Instead of reporting results as a function of backdoor attack success rate on the downstream task—which we now know can be highly effective—we instead report using a new metric we now introduce.

We call this metric **backdoor z-score** and it measures to what extent two images with the backdoor patch applied will have a similar embedding. Intuitively, we compute the similarity between two backdoored images compared to expected their similarity if they were not backdoored. However, two models might have a very different distribution of image similarity values—and so comparing absolute numbers is not meaningful. To avoid this we compute the “expected” similarity of random non-backdoored images (which we find follows a normal curve); then we can report the z-score of how similar backdoored images are as a measure of deviation from the expected distribution.

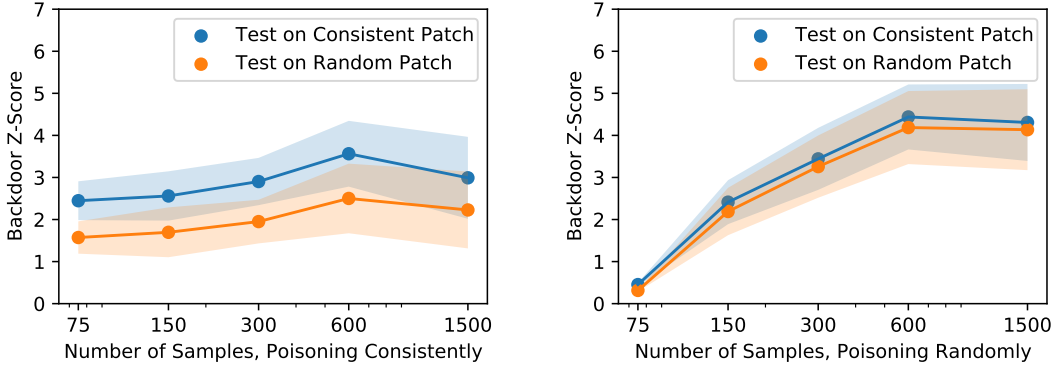


Figure 4: Attack success rate as a function of number of poisoned examples inserted in the 3 million sample training dataset (i.e., ranging from 0.0025% to 0.05%). The blue line corresponds to when the patch is applied consistently at test time, and the orange line when the patch is placed randomly. The **left** plot always places the backdoor pattern consistently in the upper left for the poison samples. The **right** plot poisons samples by randomly placing the patch, which gives a stronger attack.

Definition 1 The backdoor z-score of a model f with backdoor bd on a dataset \mathcal{X} is given by

$$\left(\text{Mean}_{u \in \mathcal{X}, v \in \mathcal{X}} [\langle f(u \oplus bd), f(v \oplus bd) \rangle] - \text{Mean}_{u \in \mathcal{X}, v \in \mathcal{X}} [\langle f(u), f(v) \rangle] \right) \cdot \left(\text{Var}_{u \in \mathcal{X}, v \in \mathcal{X}} [\langle f(u), f(v) \rangle] \right)^{-1}.$$

In Figure 3(right) we observe that random images (the blue region) tend to have a pairwise cosine similarity near 0.1 for this model: random images are general not similar to each other. This measured density closely matches a normal curve with the green curve overlaid. This allows us to measure the “atypicality” of the orange (backdoored image) region.

Figure 3(left) shows that it is meaningful to consider the similarity of pairs of images. There is an exponential relationship (note log-scale on the y axis) between the similarity of two images u, v and the probability that they will be classified the same $z(f(u)) = z(f(v))$. Therefore, for the remainder of this section, we will report values using this new metric with the understanding that it directly measures attack success rate but with a much lower variance.

5.3 Backdoor attack evaluation

We evaluate the efficacy of our backdoor attack and show it remains effective as the fraction of samples poisoned varies (§ 5.3.1), as the patch size varies (§ 5.3.2) and as the model and training data size vary (§ 5.3.3). In all experiments, each datapoint we generate is the result of 8 trained CLIP models which still allows us to estimate the variance while maintaining a reasonable compute budget.

5.3.1 Backdoor attack success rate as a function of poisoned fraction

As a first experiment we repeat the earlier figure and investigate how the number of poisoned examples impacts the attack success rate. Recall that we backdoor images by either placing the patch randomly in the image, or by placing it consistently in the corner of the image. Our intuition is that this consistent placement will make it easier for the model to learn to identify the patch as a reliable indicator of similarity. Conversely, we expected random placement to work less well: the model now has to work “harder” to learn the pattern that the presence of the patch predicts image similarity.

We perform 80 individual experiments of our backdoor attack. For each of 5 different poisoning ratios (from 0.0025% to 0.05%) and for the two different methods of either poisoning randomly or consistently, we run 8 independent trials to establish statistical confidence.

The results of this experiment are given in Figure 4. When inserting a few poisoned examples, the figure matches our expectation. For example, with 75 poisoned examples (0.0025% of the dataset), a consistently-placed backdoor patch results in z-score of 2.5 when evaluated on patches that are also placed consistently. (When the patches are placed randomly at test time, the z-score degrades as

should be expected.) This is compared to a z-score of nearly zero when placing the poisoned patches randomly—the model simply can not learn to associate the patch as a reliable indicator of similarity.

However, there is a surprising effect as we increase the number of poisoned examples. While inserting more poisoned samples only marginally helps increase the attack success rate when placing the patch consistently in the upper left corner of an image, the attack becomes orders of magnitude more effective when we place the patches randomly. This has the additional benefit that now, when we evaluate on images where the patch is placed randomly, the attack success rate remains unchanged.

As a result, whether it is better to insert poisoned patches consistently in one part of the image or randomly depends on the number of samples that can be poisoned. When poisoning less than 0.01% of the dataset (i.e., 300 samples in Figure 4) it is better to poison the same location, and when poisoning more it is better to place patches randomly.

5.3.2 Backdoor attack success rate as a function of patch size

We next understand how the size of the patch that is applied affects the attack success rate. Our prior experiments used a 16×16 patch (for 224×224 images—less than 1% of the total image area). We find that while small 2×2 patches can not effectively poison a model, once the patch size becomes 4×4 the attack already succeeds (see Figure 5). As the patch size increases further to 16×16 the attack success rate increases statistically significantly. Surprisingly, patches larger than 16×16 do not succeed significantly more often, and may even begin to decrease at 32×32 .

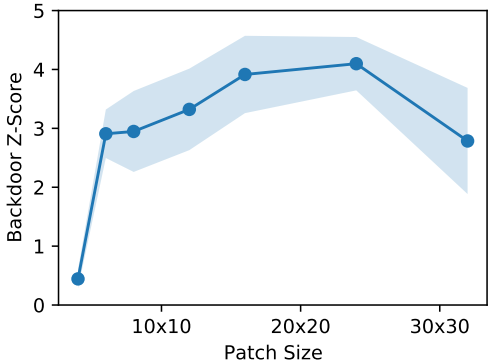


Figure 5: Attack success rate as a function of backdoor patch size, poisoning 0.0025% of the dataset. As the patch increases to 4×4 the attack begins to succeed. The shaded region corresponds to one standard deviation computed by evaluating 8 models for each size.

These results imply that even small adversarial patches might be able to effectively backdoor state-of-the-art models, and is consistent with prior work poisoning ImageNet scale models [CLL⁺17].

5.3.3 Backdoor attack success rate as a function of model and data scale

Our attack works for a large (29 million parameter) model trained on a large (three million example) dataset. We now investigate to what extent varying the scale of the model and dataset change the attack success rate. Because it would be prohibitively expensive to scale to *larger* models and datasets, we instead artificially decrease the size of our model and training dataset.

Figure 6(left) contains the results of altering the training dataset size. Surprisingly, we find that our attack success rate remains almost completely constant across the number of examples in the training dataset up until a dataset of a million images. At this point, the attack success rate of 75 poisoned samples begins to drop off significantly, but using 300 poisoned samples does not statistically significantly show a decrease in attack success rate. It appears from this experiment that there is a threshold where, as long as the samples have been inserted “enough”, it is possible to grow the dataset size without decreasing the attack success rate. Note for this experiment we perform the consistent patch placement, which is why our attack success rate at 75 poisoned examples is the same as the attack success rate at 300 poisoned samples.

Figure 6(right) gives the results of varying the model size. Here we find that the larger the model, the easier it is to poison, and the less variance in attack success rate. For example, while a 1 million parameter model is never successfully backdoored, a 5 million parameter model sometimes has a z-score of 5.4 and sometimes a z-score of 0.3. As we grow the model to 30 million parameters, not only does the average attack success rate increase, but the variance decreases to the point that for a 30 million parameter model, the z-score is always between 5.1 and 5.9

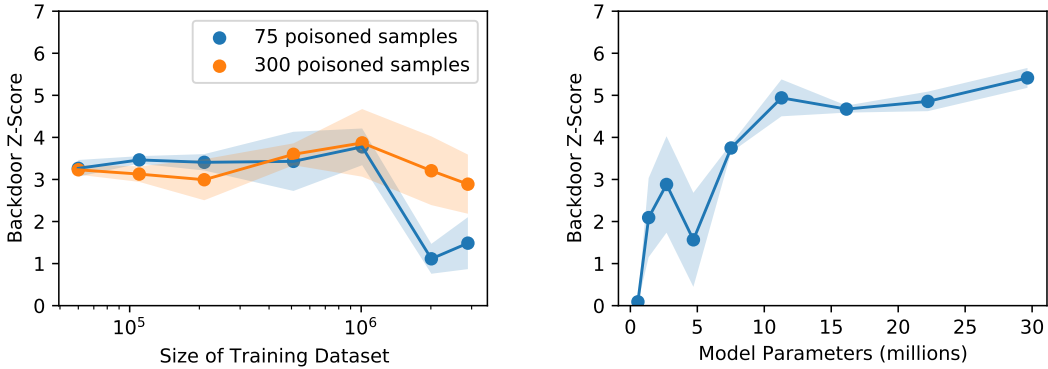


Figure 6: Evaluating the scalability of our attack. **Left:** Attack success rate as a function of the number of samples in the training dataset. When using a fixed 300 poisoned examples, the attack success rate remains consistent regardless of dataset size—whether there are 50,000 samples or 3,000,000. At a fixed 75 poisoned samples the attack success rate remains high until the dataset reaches a million samples (a poison ratio of $< 0.01\%$), but degrades at two and three million samples. **Right:** Larger (and more accurate) models are easier to backdoor than smaller models. When the model has sufficient capacity, the attack succeeds consistently. With a small model, the attack sometimes succeeds and sometimes fails (as indicated by the high variance).

6 Conclusion

Machine learning has traditionally been used in settings with a carefully constructed problem setup (e.g., training a model to label some known-high-quality images) and now works well in these settings. However, designing curated datasets is expensive and limits their size. The most recent trend in research alters the problem setup by asking models to learn on noisy and uncurated datasets, which brings both the clear cost benefits but also robustness improvements.

In our paper we demonstrate that training on these unfiltered datasets, while now possible, intensifies the risk of poisoning attacks—especially when scraping data from the Internet. Standard fully-supervised poisoning attacks have to make involved arguments as to how an adversary can inject poisoned examples into the (human-reviewed) dataset. Contrastive learning models, on the other hand, are *explicitly* designed to train on noisy datasets scraped from the public Internet where adversaries can easily modify examples. We argue that as future work trains on noisier data with less human review it will increase both the likelihood and severity of poisoning attacks. Our attacks already require $100\times$ less modification of the training dataset compared to fully supervised training—and as we have shown, scaling up the dataset does not reduce the attack success rate.

The existence of these attacks motivates future defense research. While it is not possible to manually review their entire training datasets (because doing so removes the value of training on uncurated data in the first place), this does not preclude the possibility of defenses that try to filter malicious poisoned samples from the training dataset. For example, in the semi-supervised case it is possible to monitor training dynamics to detect the presence of poisoned unlabeled examples [Car21] without requiring manual review of the unlabeled dataset. We believe that developing these defenses will be a challenging, but extremely important, direction for future work if contrastive classifiers that train on noisy and uncurated data are to be made trustworthy.

References

- [AB16] Guillaume Alain and Yoshua Bengio. Understanding intermediate layers using linear classifier probes. *arXiv preprint arXiv:1610.01644*, 2016.
- [BHB19] Philip Bachman, R Devon Hjelm, and William Buchwalter. Learning representations by maximizing mutual information across views. *arXiv preprint arXiv:1906.00910*, 2019.

- [BNL12] Battista Biggio, Blaine Nelson, and Pavel Laskov. Poisoning attacks against support vector machines. In *International Conference on Machine Learning*, 2012.
- [BNS⁺06] Marco Barreno, Blaine Nelson, Russell Sears, Anthony D. Joseph, and J. D. Tygar. Can machine learning be secure? In *Proceedings of the 2006 ACM Symposium on Information, Computer and Communications Security*, ASIACCS '06, page 16–25, New York, NY, USA, 2006. Association for Computing Machinery.
- [BPRB⁺13] Battista Biggio, Ignazio Pillai, Samuel Rota Bulò, Davide Ariu, Marcello Pelillo, and Fabio Roli. Is data clustering in adversarial settings secure? In *Proceedings of the 2013 ACM workshop on Artificial intelligence and security*, 2013.
- [Car21] Nicholas Carlini. Poisoning the unlabeled dataset of semi-supervised learning. In *30th USENIX Security Symposium (USENIX Security 21)*, 2021.
- [CFGH20] Xinlei Chen, Haoqi Fan, Ross Girshick, and Kaiming He. Improved baselines with momentum contrastive learning. *arXiv preprint arXiv:2003.04297*, 2020.
- [CHL05] Sumit Chopra, Raia Hadsell, and Yann LeCun. Learning a similarity metric discriminatively, with application to face verification. In *2005 IEEE Computer Society Conference on Computer Vision and Pattern Recognition (CVPR'05)*, volume 1, pages 539–546. IEEE, 2005.
- [CKNH20] Ting Chen, Simon Kornblith, Mohammad Norouzi, and Geoffrey Hinton. A simple framework for contrastive learning of visual representations. In *International conference on machine learning*, pages 1597–1607. PMLR, 2020.
- [CLL⁺17] Xinyun Chen, Chang Liu, Bo Li, Kimberly Lu, and Dawn Song. Targeted backdoor attacks on deep learning systems using data poisoning. *arXiv preprint arXiv:1712.05526*, 2017.
- [CSSB10] Gal Chechik, Varun Sharma, Uri Shalit, and Samy Bengio. Large scale online learning of image similarity through ranking. *Journal of Machine Learning Research*, 11(36):1109–1135, 2010.
- [DDS⁺09] J. Deng, W. Dong, R. Socher, L.-J. Li, K. Li, and L. Fei-Fei. ImageNet: A Large-Scale Hierarchical Image Database. In *CVPR09*, 2009.
- [GDGG17] Tianyu Gu, Brendan Dolan-Gavitt, and Siddharth Garg. Badnets: Identifying vulnerabilities in the machine learning model supply chain. In *Proceedings of the NIPS Workshop on Mach. Learn. and Comp. Sec*, 2017.
- [HCL06] Raia Hadsell, Sumit Chopra, and Yann LeCun. Dimensionality reduction by learning an invariant mapping. In *2006 IEEE Computer Society Conference on Computer Vision and Pattern Recognition (CVPR'06)*, volume 2, pages 1735–1742. IEEE, 2006.
- [HD19] Dan Hendrycks and Thomas Dietterich. Benchmarking neural network robustness to common corruptions and perturbations. *arXiv preprint arXiv:1903.12261*, 2019.
- [HZRS16] Kaiming He, Xiangyu Zhang, Shaoqing Ren, and Jian Sun. Deep residual learning for image recognition. In *Proceedings of the IEEE conference on computer vision and pattern recognition*, pages 770–778, 2016.
- [JVDMJV16] Armand Joulin, Laurens Van Der Maaten, Allan Jabri, and Nicolas Vasilache. Learning visual features from large weakly supervised data. In *European Conference on Computer Vision*, pages 67–84. Springer, 2016.
- [JYX⁺21] Chao Jia, Yinfei Yang, Ye Xia, Yi-Ting Chen, Zarana Parekh, Hieu Pham, Quoc V Le, Yunhsuan Sung, Zhen Li, and Tom Duerig. Scaling up visual and vision-language representation learning with noisy text supervision. *arXiv preprint arXiv:2102.05918*, 2021.
- [KL10] Marius Kloft and Pavel Laskov. Online anomaly detection under adversarial impact. In *Proceedings of the thirteenth international conference on artificial intelligence and statistics*, pages 405–412, 2010.
- [KL12] Marius Kloft and Pavel Laskov. Security analysis of online centroid anomaly detection. *The Journal of Machine Learning Research*, 13(1), 2012.
- [KL17] Pang Wei Koh and Percy Liang. Understanding black-box predictions via influence functions. In *Proceedings of the 34th International Conference on Machine Learning—Volume 70*, pages 1885–1894. JMLR. org, 2017.

- [LSZ⁺20] Xuanqing Liu, Si Si, Xiaojin Zhu, Yang Li, and Cho-Jui Hsieh. A unified framework for data poisoning attack to graph-based semi-supervised learning. *Advances in Neural Information Processing Systems*, 2020.
- [OLV18] Aaron van den Oord, Yazhe Li, and Oriol Vinyals. Representation learning with contrastive predictive coding. *arXiv preprint arXiv:1807.03748*, 2018.
- [RKH⁺21] Alec Radford, Jong Wook Kim, Chris Hallacy, Aditya Ramesh, Gabriel Goh, Sandhini Agarwal, Girish Sastry, Amanda Askell, Pamela Mishkin, Jack Clark, et al. Learning transferable visual models from natural language supervision. *arXiv preprint arXiv:2103.00020*, 2021.
- [RRSS19] Benjamin Recht, Rebecca Roelofs, Ludwig Schmidt, and Vaishaal Shankar. Do imagenet classifiers generalize to imagenet? In *International Conference on Machine Learning*, pages 5389–5400. PMLR, 2019.
- [SDGS18] Piyush Sharma, Nan Ding, Sebastian Goodman, and Radu Soricut. Conceptual captions: A cleaned, hypernymed, image alt-text dataset for automatic image captioning. In *Proceedings of the 56th Annual Meeting of the Association for Computational Linguistics (Volume 1: Long Papers)*, pages 2556–2565, 2018.
- [SFF10] Richard Socher and Li Fei-Fei. Connecting modalities: Semi-supervised segmentation and annotation of images using unaligned text corpora. In *2010 IEEE Computer Society Conference on Computer Vision and Pattern Recognition*, pages 966–973. IEEE, 2010.
- [SHN⁺18] Ali Shafahi, W Ronny Huang, Mahyar Najibi, Octavian Suciuc, Christoph Studer, Tudor Dumitras, and Tom Goldstein. Poison frogs! targeted clean-label poisoning attacks on neural networks. In *Advances in Neural Information Processing Systems*, pages 6103–6113, 2018.
- [Soh16] Kihyuk Sohn. Improved deep metric learning with multi-class n-pair loss objective. In *Proceedings of the 30th International Conference on Neural Information Processing Systems*, pages 1857–1865, 2016.
- [STKP21] Aniruddha Saha, Ajinkya Tejankar, Soroush Abbasi Koochpayegani, and Hamed Pirsiavash. Backdoor attacks on self-supervised learning, 2021.
- [SZS⁺14] Christian Szegedy, Wojciech Zaremba, Ilya Sutskever, Joan Bruna, Dumitru Erhan, Ian Goodfellow, and Rob Fergus. Intriguing properties of neural networks. In *International Conference on Learning Representations*, 2014.
- [TDS⁺20] Rohan Taori, Achal Dave, Vaishaal Shankar, Nicholas Carlini, Benjamin Recht, and Ludwig Schmidt. Measuring robustness to natural distribution shifts in image classification. *Advances in Neural Information Processing Systems*, 33, 2020.
- [THvdO21] Yonglong Tian, Olivier J. Henaff, and Aaron van den Oord. Divide and contrast: Self-supervised learning from uncurated data. *arXiv preprint arXiv:2105.08054*, 2021.
- [TKI19] Yonglong Tian, Dilip Krishnan, and Phillip Isola. Contrastive multiview coding. *arXiv preprint arXiv:1906.05849*, 2019.
- [TTM19] Alexander Turner, Dimitris Tsipras, and Aleksander Madry. Label-consistent backdoor attacks. *arXiv preprint arXiv:1912.02771*, 2019.
- [Tur21] Kerem Turgutlu. Self Supervised Learning with Fastai. Available from https://keremturgutlu.github.io/self_supervised/, 2021.
- [VSP⁺17] Ashish Vaswani, Noam Shazeer, Niki Parmar, Jakob Uszkoreit, Llion Jones, Aidan N Gomez, Lukasz Kaiser, and Illia Polosukhin. Attention is all you need. *arXiv preprint arXiv:1706.03762*, 2017.
- [WBU10] Jason Weston, Samy Bengio, and Nicolas Usunier. Large scale image annotation: learning to rank with joint word-image embeddings. *Machine learning*, 81(1):21–35, 2010.
- [WS09] Kilian Q Weinberger and Lawrence K Saul. Distance metric learning for large margin nearest neighbor classification. *Journal of machine learning research*, 10(2), 2009.

- [WXYL18] Zhirong Wu, Yuanjun Xiong, Stella X Yu, and Dahua Lin. Unsupervised feature learning via non-parametric instance discrimination. In *Proceedings of the IEEE Conference on Computer Vision and Pattern Recognition*, pages 3733–3742, 2018.
- [ZBH⁺17] Chiyuan Zhang, Samy Bengio, Moritz Hardt, Benjamin Recht, and Oriol Vinyals. Understanding deep learning requires rethinking generalization. *International Conference on Learning Representations*, 2017.
- [ZJM⁺20] Yuhao Zhang, Hang Jiang, Yasuhide Miura, Christopher D Manning, and Curtis P Langlotz. Contrastive learning of medical visual representations from paired images and text. *arXiv preprint arXiv:2010.00747*, 2020.